Subsecond regulation of striatal dopamine release by presynaptic K_{ATP} channels

Jyoti C. Patel[1], **Paul Witkovsky**[2], **William A. Coetzee**[3,4,5], and **Margaret E. Rice**[1,5]

[1]Department of Neurosurgery, New York University School of Medicine, 550 First Avenue, New York, NY 10016 USA

[2]Department of Ophthalmology, New York University School of Medicine, 550 First Avenue, New York, NY 10016 USA

[3]Department of Pediatrics, New York University School of Medicine, 550 First Avenue, New York, NY 10016 USA

[4]Department of Pharmacology, New York University School of Medicine, 550 First Avenue, New York, NY 10016 USA

[5]Department of Physiology & Neuroscience, New York University School of Medicine, 550 First Avenue, New York, NY 10016 USA

Abstract

ATP-sensitive K^+ (K_{ATP}) channels are composed of pore-forming subunits, typically Kir6.2 in neurons, and regulatory sulfonylurea receptor subunits. In dorsal striatum, activity-dependent H_2O_2 produced from glutamatergic AMPA-receptor activation inhibits dopamine release via K_{ATP} channels. Sources of modulatory H_2O_2 include medium spiny neurons, but not dopaminergic axons. Using fast-scan cyclic voltammetry in guinea-pig striatal slices and immunohistochemistry, we determined the time window for H_2O_2/K_{ATP}-channel-mediated inhibition and assessed whether modulatory K_{ATP} channels are on dopaminergic axons. Comparison of paired-pulse suppression of dopamine release in the absence and presence of glibenclamide, a K_{ATP}-channel blocker, or mercaptosuccinate, a glutathione peroxidase inhibitor that enhances endogenous H_2O_2 levels, revealed a time window for inhibition of 500 to 1000 ms after stimulation. Immunohistochemistry demonstrated localization of Kir6.2 K_{ATP}-channel subunits on dopaminergic axons. Consistent with the presence of functional K_{ATP} channels on dopaminergic axons, K_{ATP}-channel openers, diazoxide and cromakalim, suppressed single-pulse evoked dopamine release. Although cholinergic interneurons that tonically regulate dopamine release also express K_{ATP} channels, diazoxide did not induce the enhanced frequency responsiveness of dopamine release seen with nicotinic-receptor blockade. Together, these studies reveal subsecond regulation of striatal dopamine release by endogenous H_2O_2 acting at K_{ATP} channels on dopaminergic axons, including a role in paired-pulse suppression.

Keywords

Correspondence to: Dr. Margaret E. Rice or Dr. Jyoti C. Patel Dept. Neurosurgery NYU School of Medicine 550 First Avenue New York, NY 10016, USA **Telephone:** 212-263-5438 **Fax:** 212-689-0334 margaret.rice@nyu.edu or jyotiben.patel@nyumc.org.

Introduction

ATP-sensitive potassium (K_{ATP}) channels couple the metabolic state of a cell to membrane excitability (Noma 1983; Ashcroft and Ashcroft 1990; Nichols 2006). The traditional view is that they are activated primarily by ATP depletion and ADP elevation during cellular activity (Noma 1983; Findlay 1988; Ashcroft and Gribble 1998). However, K_{ATP} channels can also be activated by reactive oxygen species (ROS) that are neuronal signaling agents, including hydrogen peroxide (H_2O_2) (Avshalumov et al. 2003, 2005, 2007; Avshalumov and Rice 2003). The mechanism of H_2O_2-dependent K_{ATP} channel opening is unresolved, although there is evidence for indirect activation via ATP depletion, which is irreversible (Krippeit-Drews et al. 1999), as well as direct activation, possibly via interaction with redox-sensitive sites associated with the channels (Ichinari et al. 1996; Tokube et al. 1998).

K_{ATP} channels are octameric proteins (Clement et al. 1997; Shyng and Nichols 1997) composed of four inward rectifying pore-forming subunits, typically Kir6.2 in neurons and Kir6.1 in glia (Karschin et al. 1997; Dunn-Meynell et al. 1998; Thomzig et al. 2001), and four regulatory sulfonylurea receptor (SUR) subunits, selected from one of three subtypes: SUR1, SUR2A, or SUR2B (Shyng et al. 1997; Nichols 2006). The Kir6.2 subunit contains ATP binding sites responsible for channel inhibition, whereas SUR subunits further modulate ATP sensitivity and contain modulatory sites that are sensitive to sulfonylurea blockers, channel openers, and MgADP (Shyng et al. 1997; Nichols 2006).

Binding studies indicate that K_{ATP} channels are highly expressed in the basal ganglia, including the substantia nigra (SN) and striatum (Mourre et al. 1989; Xia and Haddad 1991; Treherne and Ashford 1991; Zini et al. 1993; Schwanstecher and Panten 1994; Dunn-Meynell et al. 1997). In dorsal striatum, activity-dependent H_2O_2 generated downstream from glutamatergic AMPA-receptor activation inhibits axonal dopamine (DA) release (Avshalumov et al. 2003; 2008; Bao et al. 2009) via the activation of SUR1-based K_{ATP} channels (Avshalumov and Rice 2003). Additional evidence indicates that modulatory H_2O_2 in striatum is not generated in dopaminergic (DAergic) axons, but is produced by mitochondria in non-DAergic cells, including medium spiny neurons (MSNs) (Avshalumov et al. 2008; Bao et al. 2009), with subsequent diffusion to K_{ATP} channels that inhibit DA release. However, the time course of this signaling has not been examined. Moreover, the question of whether DAergic axons express functional K_{ATP} channels, and are therefore direct targets of modulatory H_2O_2, remains open. Other striatal neurons, including cholinergic interneurons, are known to express K_{ATP} channels (Lee et al. 1998; Thomzig et al. 2003). Given the potent regulation of DA release by acetylcholine (ACh) acting at nicotinic ACh receptors (nAChRs) on DAergic axons (Zhou et al. 2001; Rice and Cragg 2004; Zhang and Sulzer 2004), activation of K_{ATP} channels by modulatory H_2O_2 might suppress DA release indirectly via K_{ATP} channels on striatal cholinergic cells.

Here we used fast-scan cyclic voltammetry (FCV) with carbon fiber electrodes (Patel and Rice 2006) to determine the time window of endogenous H_2O_2/K_{ATP}-dependent regulation of axonal DA release in dorsal striatum. We then used immunohistochemical and pharmacological methods to demonstrate the presence of functional K_{ATP} channels on nigrostriatal DAergic axons. Our results indicate that K_{ATP} channels intrinsic to DA axons are an integral component of a modulatory system affecting DA release in the striatum.

Materials and Methods

Animals

All animal handling procedures were in accordance with the National Institutes of Health guidelines and were approved by New York University School of Medicine's Institutional

Animal Care and Use Committee (IACUC). Young adult guinea pigs (male, Hartley, 150–250g) were obtained from Charles River (Wilmington, MA, USA). The animals were housed in groups of up to four, maintained on a 12 h light/dark cycle, and fed guinea pig chow and tap water *ad libitum* up to the time of experimentation. Housing temperature was 16–20°C.

Preparation of acute striatal slices

Animals were deeply anesthetized with sodium pentobarbital (50 mg/kg administered i.p.) and decapitated. The brain was rapidly removed and immersed for 1–2 minutes in ice-cold HEPES-buffered artificial cerebrospinal fluid (aCSF) containing (in mM): NaCl (120), KCl (5), NaHCO$_3$ (20), HEPES acid (6.7), HEPES salt (3.3), MgSO$_2$ (2), glucose (10); CaCl$_2$ (2) and saturated with 95% O$_2$/5% CO$_2$ (Rice et al. 1997; Avshalumov et al. 2008). Coronal striatal slices (400 μm thick) were prepared using a Vibratome (Ted Pella, St. Louis, MO, USA) and kept at room temperature for at least 1 h in HEPES-buffered aCSF saturated with 95% O$_2$/5% CO$_2$ before experimentation.

Voltammetric recording of evoked DA release

For studies of evoked DA release, slices were transferred to a submersion chamber (Warner Instruments LLC, Holliston, MA, USA) maintained at 32 °C and superfused at 1.2 mL/min with bicarbonate-buffered aCSF containing (in mM): NaCl (124); KCl (3.7); NaHCO$_3$ (26); MgSO$_2$ (1.3); KH$_2$PO$_4$ (1.3); glucose (10); CaCl$_2$ (2.4), equilibrated with 95% O$_2$/5% CO$_2$. Extracellular DA concentration ([DA]$_o$) evoked by local electrical stimulation was monitored in the dorsolateral striatum using FCV with carbon fiber electrodes (7 μm tip diameter, 30–50 μm length) that were either purchased from WPI Inc (Sarasota, FL, USA) or manufactured in-house (Millar and Pelling 2001; Patel and Rice 2006; Patel et al. 2009). The instrumentation for FCV was a Millar voltammeter (available by special request to Dr. Julian Millar at St. Bartholomew's and the Royal London School of Medicine and Dentistry, University of London, UK). Details of the methods and parameters used for FCV have been described elsewhere (Chen and Rice 2001). Briefly, the scan range was −0.7 V – +1.3 V (vs. Ag/AgCl), scan rate was 800 V/s, and the sampling interval was 100 ms. Identification of released DA was according to voltammograms displaying characteristic redox potentials for DA with a peak oxidation potential at typically +600 mV and a peak reduction potential at −200 mV (Patel and Rice 2006). Oxidation currents monitored during local stimulation were converted to [DA]$_o$ by post-experimental calibration of the carbon-fiber microelectrode in known concentrations of DA at 32 °C in control aCSF and in all drug-containing media used in a given experiment.

Stimulation paradigms and experimental design

A bipolar stimulating electrode used for electrical stimulation was positioned on the surface of the slice within 200 μm of the carbon-fiber recording electrode; the recording electrode was inserted 50–100 μm into the tissue. Following a 30 min equilibration period, DA release was evoked, using square wave pulses (0.6–0.8 mA pulse amplitude, 0.1 ms pulse duration) controlled by a Master 8 pulse stimulator and Isoflex stimulus isolator (A.M.P.I., Jerusalem, Israel). Four stimulation paradigms were used to address different experimental questions: paired pulses, single stimulation pulses, brief 5-pulse stimulation trains, and 30-pulse trains.

To determine the time course of H$_2$O$_2$/K$_{ATP}$ channel regulation of DA release, we used a paired-pulse paradigm consisting of a pseudo-one-pulse stimulus (P1; 10 pulses at 100 Hz) to elicit DA release and concurrent H$_2$O$_2$ generation, followed at varying time intervals (250 ms to 2000 ms) by a single test pulse (P2). The amplitude of [DA]$_o$ evoked by P2 was determined by subtracting P1 alone from the summed [DA]$_o$ record, P1+P2. In these experiments, the DA D2 receptor antagonist (−)sulpiride (1 μM) was included in the

superfusion buffer for at least 40 to 50 min before recording to eliminate confounding inhibitory effects of D2 autoreceptor activation on paired-pulse evoked $[DA]_o$ (Phillips et al. 2002). It should be noted that (−)sulpiride does not interfere with K_{ATP}-channel activation (see Results) or with H_2O_2-dependent modulation of axonal DA release (Avshalumov and Rice 2003). Following preincubation with sulpiride, stimulations were then applied at 5 min intervals. Initially, 4–5 consistent P1 responses were obtained, then the P1+P2 stimulation sequences were initiated using intervals between P1 and P2 of 250, 500, 1000, 1500 or 2000 ms. The stimulation sequence was presented in alternating ascending or descending order to minimize experimental bias. After the last P1+P2 stimulus, P1 evoked $[DA]_o$ alone was again assessed and averaged with the pre-sequence value; this average was used as control P1 for a given recording site. The procedure was then repeated in the presence of a drug to test the involvement of K_{ATP} channels and H_2O_2.

Single-pulse (1 p) stimulation applied at 5 min intervals was used to determine whether K_{ATP} channel openers have a direct action on DA axons. This stimulus offers the advantage of evoking axonal DA release in dorsal striatum that is free from inhibition by endogenous DA acting at D2 autoreceptors (Limberger et al. 1991; Patel et al. 1992; Trout and Kruk 1992; Phillips et al. 2002) and from modulation of DA by concurrently released glutamate or GABA (Avshalumov et al. 2003; Chen et al. 2006). Under control conditions, peak 1 p evoked $[DA]_o$ is stable for at least 3 h when applied at 5 minute intervals (Bao et al. 2005). After 4–5 consistent responses were obtained in control conditions, a given drug was applied until its effect on peak evoked $[DA]_o$ reached a plateau, usually within 45 minutes. Drug effects were quantified as the percent change of the averaged response prior to drug application.

Lastly, to examine possible involvement of K_{ATP}-channel-mediated inhibition of cholinergic input to DAergic axons two pulse-train stimulation paradigms were used. The first was a series of 5-pulse (5 p) trains (10, 25 and 100 Hz) applied at 5 min intervals. This approach is based on the enhanced frequency response seen in striatal slices when nAChRs are blocked (Rice and Cragg 2004; Zhang and Sulzer 2004; Bao et al. 2010). In these experiments, the frequency dependence of peak evoked $[DA]_o$ obtained in the presence of a K_{ATP} channel opener was compared with that seen with the nAChR antagonist mecamylamine. The frequency response was determined at three sites in a given slice either under control conditions or in the presence of the drug tested in a paired slice. Stimulation frequencies were presented in random order in the first slice, with the same order of stimulation repeated in the paired slice. The average of peak 1 p evoked $[DA]_o$ before and after pulse-train application was used to calculate the ratio of 5 p to 1 p evoked $[DA]_o$ as a measure of frequency responsiveness. Data are presented as absolute $[DA]_o$ or 5 p to 1 p ratio. The second pulse-train paradigm was a 10 Hz, 30 pulse train applied at 10 min intervals to evoke release of DA, under conditions that allow examination of glutamate-dependent H_2O_2 generation (Avshalumov et al. 2003, 2008). In these experiments, 3–4 stable DA release records were obtained then a drug (or drug combination) was applied via superfusion in aCSF. Data are expressed as percentage of the averaged control response before drug application.

Western Blots

Guinea pigs were deeply anesthetized with sodium pentobarbital (50 mg/kg administered i.p.), then transcardially perfused with ice-cold solution containing (in mM): 225 sucrose, 2.5 KCl, 0.5 $CaCl_2$ 7 $MgCl_2$, 28 $NaHCO_3$ 1.25 NaH_2PO_4, 7 glucose, 1 ascorbate and 3 pyruvate, equilibrated with 95% O_2/5% CO_2 (Avshalumov et al. 2008). The brain was quickly removed, a sample of striatal tissue (~50 mg) excised and placed in 200 μL Protease Inhibitor (Sigma-Aldrich) in a microcentrifuge tube, sonicated then centrifuged at 12,000 rpm for 10 min at 4°C. The supernatant was removed, with 10 μL reserved for protein

determination by the bicinchoninic acid protein assay (Sigma-Aldrich), and the balance diluted 1:1 in Laemmle buffer with 5% v/v ß-mercaptoethanol. Proteins were resolved by 10% SDS-PAGE and detected by Western blotting. Proteins were transferred to nitrocellulose membranes and blocked with 5% fat-free milk and 0.05% Tween 20 in Tris-buffered saline (TBS; 200 mM NaCl, 0.1 M Tris buffer, pH 7.4) for 1 h at room temperature. Primary and secondary antibodies were dissolved in TBS containing 5% milk and 0.05% Tween and membranes were incubated with primary antibody for 1h. The secondary antibody used was a horseradish peroxidase-linked anti-biotin rabbit antibody (Cell Signaling Technology, Inc., Danvers, MA). Chemiluminescent Western blotting substrate (Pierce, Rockford, IL, USA) was used for peroxidase detection and the resulting signal was detected on Kodak Biomax light films (Sigma-Aldrich). The molecular mass of proteins was estimated by reference to a biotinylated protein ladder (Cell Signaling Technology, Inc.).

Immunohistochemistry

The methods used for immunohistochemistry were similar to those described previously (Patel et al. 2009). Guinea pigs were deeply anesthetized with sodium pentobarbital (50 mg/kg, i.p.), then perfused transcardially with room temperature phosphate-buffered saline (PBS; 9.0 g/L NaCl in 10 mM phosphate buffer, pH 7.2) followed by freshly prepared 4% paraformaldehyde in PBS. After the brain was removed, the striatum was blocked in the sagittal plane and post-fixed in 4% paraformaldehyde in PBS for 1 h at room temperature, then the block was washed successively for 30 min each in 10%, and 20% sucrose in PBS. After 12–16 h in 30% sucrose in PBS at 4 °C, sagittal sections of the striatum (20 μm) were cut on a Reichert-Jung Cryocut 1800 cryostat (Belair Instrument Company, Springfield, NJ), mounted on SuperFrost slides (Fisher Scientific, Pittsburgh PA), dried for 1h at 37 °C, and stored frozen until used.

For immunostaining, brain sections were thawed, washed 3 times for 6 min (3 × 6 min) in PBS, then placed for 30 min in blocking solution [10 mL PBS, 30 μL Triton-X 100, 100 mg bovine serum albumin (Sigma, St. Louis MO), 10% w/v Na azide solution (Sigma)]. Primary and secondary antibodies were diluted in blocking solution. Primary antibodies were applied for 2 h at room temperature, followed by 3 × 6 min washes in PBS, then secondary antibodies applied for 1 h at room temperature, followed by 3 × 6 min washes in PBS. After the final set of washes, sections were coverslipped in VectaShield (Vector Labs, Burlingame CA).

Striatal DAergic axons were identified using two anti-tyrosine hydroxylase (TH) antibodies: AB152 rabbit anti-TH (1:800) and MAB318 mouse anti-TH (1:500) (both from Chemicon, Temecula, CA). Polyclonal AB152 was raised against denatured TH from rat pheochromocytoma and MAB319 raised against purified TH from PC12 cells; both anti-TH antibodies immunostain DAergic neurons in brain (Patel et al. 2009; Witkovsky et al. 2009). Immunohistochemical localization of K_{ATP} channels in the striatum was assessed using three different primary antibodies against Kir6.2: NBP1-00900 rabbit anti-Kir6.2 (1:100) (Novus Biologicals, Littleton, CO); chicken anti-Kir6.2 (1:100) (C62; developed by the Coetzee group against peptide Ac-CVAKAKPKFSISPDSLS-amide) and rabbit anti-Kir6.2 (hereafter LL; 1:300) (Lu et al. 2006; a kind gift from Dr. Hon-Chi Lee, Mayo Clinic, Minnesota). Both the C62 and LL anti-Kir6.2 antibodies detect a ~37 kDa band in immunoblots obtained with lysates from HEK-293 cells stably transfected with Kir6.2/SUR1 subunits (not shown). No cross-reactivity was observed when tested against lysates from Kir6.1/SUR2B stably transfected HEK-293 cells (not shown). The C62 anti-Kir6.2 antibody also labeled a ~37 kDa band in Western blots of guinea-pig brain tissue (see below). The specificity of the remaining rabbit anti-Kir6.2 antibody (NBP1-00900) was validated by the similar immunostaining patterns of guinea-pig striatum when compared

with the C62 or LL anti-Kir6.2 antibodies (see below). Secondary antibodies used were donkey anti-mouse Alexa 488 (Invitrogen, Carlsbad, CA), Cy3-conjugated donkey anti-chicken and Cy3-conjugated donkey-anti rabbit (Jackson Laboratory, Bar Harbor, ME).

Image Processing

Immunofluoresence images were obtained with a Nikon PM 800 confocal microscope equipped with a digital camera controlled by Spot software (Diagnostic Instruments Inc., Sterling Heights, MI). Digital images were acquired separately from each laser channel, then combined. Digital files were processed with deconvolution software (AutoQuant Imaging, Watervliet, NY). Final images were processed using Adobe Photoshop 7.0 (Adobe, San Jose, CA). All images were adjusted for brightness and contrast; such adjustments were made uniformly to all parts of the image.

Drugs and Chemicals

All experimental solutions were prepared immediately before use. Components of the HEPES- and bicarbonate-buffered aCSF and all perfusion solutions were purchased from Sigma-Aldrich Chemical Co. (St. Louis, MO). Glibenclamide (purchased as glybenclamide), mercaptosuccinate (MCS; purchased as mercaptosuccinic acid), mecamylamine and DA were also obtained from Sigma-Aldrich. Diazoxide, cromakalim, (−)sulpiride, and quinpirole were purchased from Tocris Bioscience (Ellisville, MO). MCS, mecamylamine and quinpirole were dissolved directly in aCSF. Stock solutions of glibenclamide, diazoxide, and cromakalim in DMSO were diluted in aCSF immediately before use; the final DMSO concentration did not exceed 0.4% (v/v). When these drugs were used, control responses were obtained in the presence of DMSO at the same concentration used with the drug.

Statistical analysis

Data were analyzed using Prism Software (GraphPad, San Diego, CA). Data are expressed as means ± SEM, where n equals the number of slices or recording sites for FCV (as indicated in the text) and presented as absolute $[DA]_o$, the ratio of 5 p to 1 p evoked $[DA]_o$, or percent of pre-drug control. Significance of differences was assessed using unpaired Student's t-tests, one- or two-way ANOVA (indicated either in the text or figure legends), as appropriate. The confidence level for significance was 95%.

Results

Time course of H_2O_2-dependent K_{ATP}-channel activation

To determine the time course of striatal DA release suppression by modulatory H_2O_2 and K_{ATP} channel activation, we used a paired-pulse paradigm in which the influence of endogenous H_2O_2 generated during an initial stimulus (P1) was assessed on $[DA]_o$ evoked by a subsequent test pulse (P2) applied at varying interpulse intervals. Under control conditions in dorsal striatum, P2 is always smaller than P1 at interpulse intervals of <30 s, even when D2 DA autoreceptors are blocked, because of several factors, including depletion of the releasable DA pool, strong cholinergic regulation of initial DA release, and other as yet undefined factors (Lee et al. 2002; Phillips et al. 2002; Cragg 2003; Rice and Cragg 2004; Zhang and Sulzer 2004). The amplitude of P2 was determined by subtracting P1 from P1+P2 at intervals up to 2000 ms under varying experimental conditions (Fig. 1A,B). To assess the role of inhibitory K_{ATP} channels in striatal paired-pulse suppression, we repeated the basic paradigm in the presence of a K_{ATP} channel blocker, glibenclamide (3 μM; Bao et al. 2005) (Fig. 1B, Fig. 2). Supporting a role for K_{ATP}-channel activation in striatal paired-pulse suppression, comparison of peak P2 $[DA]_o$ amplitude over time showed significantly less attenuation in the presence of the K_{ATP}-channel blocker glibenclamide than in control

conditions ($p < 0.01$, two-way ANOVA) (Fig. 2). This experiment also revealed the time course of K_{ATP} channel activation, with no effect 250 ms after P1, a significant increase in P2 amplitude 500 ms and 1000 ms after P1, and a return to control values by 1500 ms after P1 (Fig. 2)

To assess the role of endogenously produced H_2O_2 in striatal paired-pulse suppression, we amplified locally generated H_2O_2 by inhibiting glutathione (GSH) peroxidase with mercaptosuccinate (MCS, 1 mM) (Avshalumov et al. 2003, 2004, 2008). Previous studies demonstrated that H_2O_2-dependent inhibition of evoked $[DA]_o$ is K_{ATP}-channel-dependent (Avshalumov et al. 2003, 2005; Avshalumov and Rice 2003; Bao et al. 2005). Comparison of P2 amplitude over time in the presence and absence of MCS indicated an enhancement of paired-pulse suppression in MCS *versus* control ($p = 0.05$, two-way ANOVA) (Fig. 2). The time course of H_2O_2-dependent modulation of evoked DA release was the same as that seen with K_{ATP} channel blockade: P2 amplitude was unchanged 250 ms after P1, was suppressed at 500 ms and 1000 ms, then returned to control by 1500 ms after P1 (Fig. 2). Collectively, these data indicate rapid, transient suppression of axonal DA release by H_2O_2-dependent, K_{ATP}-channel activation in dorsal striatum.

Evidence for anatomical localization of K_{ATP} channels on striatal DAergic axons

A straightforward explanation for rapid, reversible inhibition of striatal DA release by H_2O_2 is that the K_{ATP} channels mediating this effect are located directly on DAergic axons (Avshalumov et al. 2008). Western blot analysis confirmed expression of Kir6.2 in striatal tissue. The C62 anti-Kir6.2 antibody stained a primary band at ~37 kDa, with an additional minor band at ~22 kD (Fig. 3). The 37 kDa band corresponds closely to that reported previously for Kir6.2 expression in stably transfected HEK-393 cells (Morrissey et al. 2005). Neither NBP1-00900 nor LL anti-Kir6.2 effectively detected these bands when striatal tissue was analyzed with Western blotting.

To determine whether K_{ATP} channels are localized on DAergic axons, we used immunohistochemical methods with antibodies to TH (Witkovsky et al. 2009; Patel et al. 2009), a DA synthesizing enzyme, and to Kir6.2, which is the pore-forming subunit of all K_{ATP} channels in SNc DAergic neurons (Liss et al. 1999). Striatal axons that were TH immunoreactive (TH-ir) showed uniform labeling throughout (Fig. 4A). By contrast, Kir6.2 staining was invariably punctate (Fig. 4B). These immunostained puncta appeared as individual or aggregated grains over the general region of TH-ir axons (Fig. 4C). In planes of section that contained extended TH-ir axons or axon bundles, co-localization of Kir6.2-ir puncta was clearly seen (Fig. 4D–F). Additionally, Kir6.2 puncta were sometimes organized into clumps of high grain density in ovoid regions, 20–40 µm in long axis, but lacking TH staining, which may represent association of Kir6.2 with perikarya of non-DAergic striatal neurons (Fig. 4). Identification of these cells was not pursued. Similar patterns of staining were seen with all three anti-Kir6.2 antibodies tested; figure legends indicate which was used for a given image.

We then sought to confirm the presence of Kir6.2-ir puncta in TH-ir axons more quantitatively. Our initial experiments indicated that individual Kir6.2-ir puncta were either dense or pale. We considered two possibilities for this difference: 1) pale puncta were dense puncta that were out of focus; or 2) pale puncta reflected non-specific background staining. To distinguish between these, we made serial *z*-stack images at 0.2 µm thickness through a 2.0 µm depth to assess whether individual puncta changed optical density with depth. They did not; dense puncta remained dense and pale ones never became dense. On this basis, we concluded that only dense puncta represented Kir6.2 subunits. Subsequently, to eliminate pale puncta from images used to assess co-localization of TH and Kir6.2, we set an adjustable threshold step in NIH Image J. We then used black/white reversal to render TH-ir

processes white and superimposed TH and Kir6.2immunostained images in Photoshop, with the opacity of the Kir6.2 image adjusted to 50–60% to yield a final overlay image (Fig. 5).

Kir6.2-ir puncta were distributed generally throughout these adjusted images, indicating that superimposition with a TH-ir profile will, to some degree, occur by chance. To test this assumption, we counted Kir6.2/TH superpositions for each image (Fig. 5A,C). Then the Kir6.2 digital files were rotated 90° clockwise and the counts repeated (5B,D); for all fields, rotation decreased the number of Kir6.2-ir puncta that colocalized with TH. In these images, Kir6.2-ir puncta that did not colocalize with TH are black, whereas superimposed puncta appear dark gray (Fig. 5). This procedure was repeated for six test fields; in each case, rotation resulted in a fall in the number of superpositions (mean difference aligned *vs.* rotated was $-29.4 \pm 2.9\%$; n = 6; $p < 0.01$ paired t-test) (Table 1). This finding indicates that at least 30% of Kir6.2-ir puncta in each striatal field are located on DAergic axons.

As a second test of whether superpositions occurred only at chance levels, we selected images showing a range of TH-ir process density. The percent of total area covered by TH-ir processes and the density of Kir6.2-ir puncta were calculated using Image J. For this analysis, we counted only puncta that were 5–75 pixels in area, which encompassed the dimensions of individual puncta, but excluded aggregates. The resulting plot of Kir6.2-ir puncta density *versus* percent TH-ir coverage showed a positive correlation between these two measures (Fig. 5E), confirming that Kir6.2-ir puncta are associated with DAergic axons in guinea-pig striatum.

Evidence for functional K_{ATP} channels on striatal DAergic axons

Our immunohistochemical data demonstrate the presence of K_{ATP} channels on striatal DAergic axons. We then investigated whether these channels are involved in DA release modulation by examining the effect of pharmacological manipulation of K_{ATP}- channels on 1 p evoked DA release. We first used the K_{ATP}-channel blocker glibenclamide to establish whether K_{ATP} channels tonically inhibit axonal DA release under resting conditions. Glibenclamide (3–10 μM) did not alter $[DA]_o$ evoked by single-pulse stimulation ($94 \pm 4\%$ control, $p > 0.05$ vs. same-site control, n = 7) indicating the absence of tonic regulation mediated by K_{ATP}-channels *in vitro* (not illustrated).

We next tested whether K_{ATP}-channel openers inhibited single-pulse evoked $[DA]_o$, which would be consistent with a direct effect on DAergic axons. SUR1- and SUR2-based K_{ATP} channels can be distinguished to a certain extent by their differential sensitivity to channel openers (Inagaki et al. 1996; Babenko et al. 2000; Avshalumov et al. 2005; Glukhov et al. 2010). Here we assessed the effect of the one known opener of SUR1 channels, diazoxide (30–60 μM), or SUR2-selective cromakalim (30–60 μM) individually, then added the other opener to test whether the actions of each were additive or occlusive. This experimental design also took into account the possible lack of specificity of these drugs, e.g., evidence for activation of SUR2B-, as well as SUR1-based K_{ATP} channels by diazoxide in muscle cells (Isomoto et al. 1996). We found that diazoxide alone caused an average 38% decrease in 1 p evoked $[DA]_o$ (n = 6) (Fig. 6A,C). Similarly, cromakalim alone decreased 1 p evoked $[DA]_o$ by 26% (n = 6) (Fig. 6B,C). The magnitude of DA release suppression by diazoxide or cromakalim alone did not differ statistically ($p > 0.05$; n = 6). Notably, diazoxide also caused a significant decrease in 1 p evoked $[DA]_o$ in the presence of cromakalim (n = 6, $p < 0.05$ cromakalim *vs.* cromakalim + diazoxide) (Fig. 6B,C), and cromakalim caused a significant decrease in the presence of diazoxide (n = 6, $p < 0.05$ diazoxide *vs.* diazoxide + cromakalim) (Fig. 6A,C), suggesting that SUR1- and SUR2-based K_{ATP} channels independently regulate striatal DA release in guinea-pig striatum.

Are cholinergic interneurons involved in H_2O_2/K_{ATP}-channel dependent suppression of DA release?

Suppression of 1 p evoked DA release by K_{ATP}-channel openers is consistent with a direct effect on DAergic axons. An alternative explanation, however, is that release suppression reflects an indirect consequence of altered cholinergic tone via activation of K_{ATP} channels on cholinergic interneurons (Lee et al. 1998; Thomzig et al. 2003), given the strong regulation of axonal DA release by tonic activation of nAChRs that are expressed on DAergic axons (Zhou et al. 2001; Rice and Cragg 2004; Zhang and Sulzer 2004). When nAChRs are blocked, 1 p evoked $[DA]_o$ is suppressed, but the frequency responsiveness is amplified (Rice and Cragg 2004; Zhang and Sulzer 2004; Bao et al. 2010). We therefore first examined whether the suppression of 1 p evoked $[DA]_o$ by diazoxide was accompanied by an increase in the response to 5 p trains at frequencies of 10, 25, and 100 Hz, as seen with a sub-maximal concentration of mecamylamine (500 nM), a nAChR antagonist (Fig. 7). Diazoxide was examined because previous studies indicate that striatal cholinergic neurons express only SUR1-based K_{ATP} channels (Lee et al. 1998; Thomzig et al. 2003). As reported previously (Rice and Cragg 2004; Zhang and Sulzer 2004; Bao et al. 2010), mecamylamine not only caused suppression of $[DA]_o$, evoked by 1 p, but also induced a significant frequency dependence of release with 5 p trains that was absent under control conditions (n = 9 sites) (Fig. 7A,C,D). Activation of K_{ATP} channels by diazoxide (60 μM) also suppressed $[DA]_o$ evoked by 1 p; however in contrast to the effect of mecamylamine, a similar level of suppression was seen with 5 p trains across all frequencies tested (Fig. 7B,E), with no change in the frequency-dependence of striatal DA release ($p > 0.05$ for all frequencies, n = 9 sites) (Fig. 7F). These data imply a lack of involvement of cholinergic interneurons in the effect of K_{ATP} channels on striatal DA release.

To test whether H_2O_2-induced inhibition of axonal DA release is also independent of effects on cholinergic tone, we examined whether the effect of nAChR blockade by mecamylamine on pulse-train evoked $[DA]_o$ (30 p, 10 Hz) was occluded when endogenously generated H_2O_2 levels were amplified by MCS. Because blockade of nAChRs with mecamylamine causes progressive rundown of $[DA]_o$ evoked by repetitive 3 s pulse-train stimulations (unpublished observations), it was not possible to assess whether endogenous H_2O_2-dependent DA release regulation could be prevented by mecamylamine. We therefore tested this using the opposite approach. Consistent with the inhibitory effect of nAChR blockade on low frequency-evoked DA release (e.g., Fig. 7C), mecamylamine (5 μM) caused a ~30% suppression of pulse-train evoked $[DA]_o$ (30 p, 10 Hz) after 5 min application ($p < 0.001$, n = 5) (Fig. 8A,C). Amplification of H_2O_2 by MCS (1 mM) caused a ~35% suppression of pulse-train evoked $[DA]_o$ (Fig. 8B,C), shown previously to be K_{ATP}-channel dependent (Avshalumov et al. 2003; Avshalumov and Rice 2003). In the continued presence of MCS, mecamylamine caused a further suppression of pulse-train evoked $[DA]_o$ after 5 min (Fig. 8B,C). The magnitude of this decrease was indistinguishable from to that observed in the absence of MCS (Fig. 8C), implying a lack of involvement of altered ACh release in DA release regulation by endogenous H_2O_2.

Suppression of DA release by K_{ATP}–channels is independent of DA D2 autoreceptors

Early studies showing prevention of D2 receptor-mediated hyperpolarization of SNc DAergic neurons by glibenclamide (Roeper et al. 1990; Lin et al. 1993) suggested a possible interaction between K_{ATP} channels and D2 DA autoreceptor-activated GIRK (G-protein-activated inward rectifier K^+) channels. We reported previously that MCS-induced suppression of pulse-train evoked DA release was unaffected by blockade of D2 receptors by sulpiride (Avshalumov and Rice 2003). However, in those studies, possible D2/K_{ATP}-channel interaction on presynaptic DAergic axons was not tested directly using K_{ATP} channel openers or blockers. Here we addressed this limitation by examining the effect of a

D2 receptor agonist on 1 p evoked $[DA]_o$ in the absence and presence of glibenclamide and by examining the effects of diazoxide and cromakalim in the presence of sulpiride, (Fig. 9). Quinpirole (100 nM), a D2 receptor agonist, caused a ~50% inhibition of 1 p evoked DA release (Fig. 9A,C), with a similar level of inhibition in the presence of glibenclamide (3–10 μM) ($p > 0.05$ quinpirole *vs.* quinpirole + glibenclamide, n = 6) (Fig. 9B,F). Moreover, in the presence of sulpiride (1 μM), both diazoxide (60 μM) and cromakalim (60 μM) suppressed single pulse evoked $[DA]_o$ (Figure 9D–F) to the same extent seen for each in the absence of sulpiride (compare Figs. 9F and 6C; $p > 0.05$ for each, n = 6). These data support the independence of K_{ATP}-channel dependent suppression of axonal DA release and that mediated by presynaptic D2 autoreceptors.

Discussion

Although ROS in the brain are often viewed at best as unwanted by-products of oxidative metabolism, and at worst as neurotoxins, increasing evidence indicates that these substances are signaling agents in the brain under physiological conditions. In particular, H_2O_2 has been shown to regulate K_{ATP} channels in the nigrostriatal DAergic pathway in an activity-dependent manner (Avshalumov et al. 2003, 2005, 2008). Previous studies showed that H_2O_2/K_{ATP}-channel dependent modulation of evoked $[DA]_o$ affects release, with no effect on DA uptake via the DA transporter (Avshalumov and Rice 2003). We report here the first evaluation of the time course of activity-dependent inhibition of striatal DA release, which revealed significant subsecond regulation by K_{ATP} channels and H_2O_2. Using immunohistochemistry, we demonstrated the presence of K_{ATP} channels on DAergic axons in guinea-pig dorsal striatum. These data support our working hypothesis that modulatory H_2O_2 inhibits DA release through activation of presynaptic K_{ATP} channels on DAergic axons. This hypothesis was bolstered by the results of functional experiments demonstrating that K_{ATP}-channel openers inhibit 1 p evoked DA release in dorsal striatum. We also disproved alternative hypotheses that DA release suppression might be either an indirect consequence of K_{ATP} channel activation on cholinergic interneurons or through competition with D2 DA autoreceptors. Collectively, these data show that H_2O_2-dependent activation of K_{ATP} channels on DAergic axons provides direct, transient inhibition of axonal DA release on a subsecond time scale.

Subsecond regulation of axonal DA release by endogenous H_2O_2 and K_{ATP} channels

Previous studies of H_2O_2/K_{ATP}-channel-dependent modulation of striatal DA release have demonstrated that H_2O_2 generation occurs downstream from AMPAR activation, primarily in MSNs (Avshalumov et al. 2003, 2008; Avshalumov and Rice 2003; Bao et al. 2009). Evidence for this includes the findings that: 1) the usual suppression of pulse-train evoked DA release seen when endogenous H_2O_2 levels are amplified by MCS is lost when AMPARs are blocked by GYKI-52466, indicating that modulatory H_2O_2 is AMPAR dependent (Avshalumov et al., 2003); 2) conversely, the usual increase in pulse-train evoked DA release seen with AMPAR blockade is prevented by the presence of exogenous GSH peroxidase or K_{ATP} channel blockers, indicating that its actions require H_2O_2 and K_{ATP} channels (Avshalumov et al. 2003; Avshalumov and Rice 2003); 3) activity dependent generation of H_2O_2 visualized using fluorescence imaging in MSNs is completely prevented by AMPAR blockade (Avshalumov et al. 2008); and 4) blockade of mitochondrial H_2O_2 generation by a cocktail of mitochondrial agents also prevents the usual effect of AMPAR blockade on DA release, indicating that the source of AMPAR-dependent H_2O_2 is mitochondrial respiration (Bao et al. 2009).

These earlier studies of H_2O_2-dependent modulation of DA release also provided indirect evidence that the process is relatively fast: a decrease in evoked $[DA]_o$ *versus* control is seen within the first few hundred milliseconds of pulse-train stimulation when endogenously

generated H_2O_2 is amplified by MCS (Avshalumov et al. 2003, 2008). A similarly rapid increase in evoked $[DA]_o$ relative to control is seen when K_{ATP}-channels are blocked by glibenclamide (Avshalumov et al. 2003; Avshalumov and Rice 2003). However, the present studies provide the first systematic approach to determine the dynamic window for H_2O_2/ K_{ATP}-channel-dependent modulation of striatal DA release. Using a paired-pulse paradigm similar to that used to determine the time course of D2 autoreceptor regulation of striatal DA release (Phillips et al. 2002), we discovered that the window for H_2O_2/K_{ATP}-channel-dependent regulation of DA release is from 500–1000 ms after a burst of activity, with return to control by 1500 ms.

The delay in the onset of DA release regulation, i.e., no effect on P2-evoked $[DA]_o$ amplitude at intervals <500 ms after P1, presumably reflects a number of contributing factors, including the time required for glutamate-AMPAR-dependent H_2O_2 generation and diffusion of modulatory H_2O_2 from the site of generation, including MSNs, to DAergic axons (Avshalumov et al. 2008), as well as the time required for K_{ATP}-channel activation. Analogously, termination of action within 1500 ms after P1 could reflect diffusion of modulatory H_2O_2 away from the site of generation and action, degradation of H_2O_2 by endogenous peroxidases, and the time required for K_{ATP} channel closure. The finding that inhibition of GSH peroxidase by MCS neither hastened the onset nor prolonged the duration of H_2O_2-dependent DA release regulation suggests that H_2O_2 metabolism is not a major factor in the regulatory time window. On the other hand, enhancement of the degree of DA release inhibition by MCS indicates that this process is graded in efficacy. Thus, the pattern of influence that glutamatergic input to the striatum exerts on DA release will vary according to the timing and intensity of this input with coincident activity of the nigrostriatal pathway.

Striatal DAergic axons express K_{ATP} channels

Previous binding studies using K_{ATP} channel blockers implied the presence of these channels in the nigrostriatal pathway (Mourre et al. 1989; Xia and Haddad 1991; Treherne and Ashford 1991; Zini et al. 1993; Schwanstecher and Panten 1994; Dunn-Meynell et al. 1997). More specific evaluation of mRNA for K_{ATP} channel subunits confirmed expression of Kir6.2, SUR1, and SUR2B subunits in DAergic neurons of mouse SNc during development (Liss et al. 1999). Whether the anatomical substrate of K_{ATP} channel binding sites in the striatum included nigrostriatal DAergic axons had not been addressed until the present studies, in which we evaluated co-localization of Kir6.2 and TH in guinea-pig striatum. In this proof-of-concept study, we chose to use immunohistochemical localization of Kir6.2, the pore-forming subunit of K_{ATP} channels in nigrostriatal DA projection neurons (Liss et al. 1999, 2005), rather than SUR1 or SUR2 subunits because we wanted to label all K_{ATP} channels in nigrostriatal DA axons. Our results indicate not only that striatal DAergic axons and axon bundles express Kir6.2-ir puncta, but also that this localization accounts for a high proportion, 30%, of previously reported striatal K_{ATP} channel binding sites. Localization of K_{ATP} channels on DAergic axons provides direct targets for H_2O_2-dependent inhibition of axonal DA release in dorsal striatum (Avshalumov et al. 2003, 2005, 2007, 2008; Bao et al. 2005, 2009). Unsurprisingly, Kir6.2-ir puncta were also seen in cells and processes that were not TH-ir. Identification of these Kir6.2-ir sites was beyond the scope of the present report; however, previous anatomical and functional data implicate striatal MSNs as a likely Kir6.2-ir neuron population (e.g., Schwanstecher and Panten 1994; Calabresi et al. 1999; Centonze et al. 2001; Bao et al. 2005). On the other hand, the pore-forming K_{ATP} channel subunit in cholinergic interneurons is Kir6.1 (Lee et al. 1998; Thomzig et al. 2003), as is that generally found in glia (Thomzig et al. 2001), indicating that these cell populations would not contribute to the Kir6.2 immunostaining patterns reported here.

Inhibition of axonal DA release by SUR1- and SUR2-based K$_{ATP}$ channels

Previous studies show that DAergic neurons of the SN pars compacta (SNc) in guinea-pig midbrain express K$_{ATP}$ channels that are tonically activated by H$_2$O$_2$ and thereby regulate DAergic neuron firing rate (Avshalumov et al. 2005). In those studies, sensitivity to elevated H$_2$O$_2$ was found to differ between two populations of DAergic neurons, with higher sensitivity conferred by SUR1- *versus* SUR2-based K$_{ATP}$ channels. Neurons that responded to moderate H$_2$O$_2$ elevation hyperpolarized with SUR1-acting diazoxide, but not SUR2-acting cromakalim, with the opposite patterns in nonresponsive DAergic cells, at the same concentrations of these openers used here (Avshalumov et al. 2005). Thus, guinea-pig SNc DAergic neurons exhibit segregation of SUR1-and SUR2-containing K$_{ATP}$ channels (Avshalumov et al. 2005).

Analogous evidence from guinea-pig dorsal striatum suggests the possibility of separate populations of SUR1- and SUR2-based K$_{ATP}$ channels on DAergic axons as well, with suppression of pulse-train evoked [DA]$_o$ by either diazoxide or cromakalim (Avshalumov et al. 2003). However, the use of pulse-train stimulation in those studies precluded assessment of whether these responses were mediated by K$_{ATP}$ channels located on DAergic axons or elsewhere in the local microcircuitry. Here we examined the effect of these openers on 1 p evoked DA release, which is not modulated by concurrent activation of glutamate, GABA, or D2 autoreceptors (Limberger et al. 1991; Patel et al. 1992, Trout and Kruk 1992; Philips et al. 2002; Avshalumov et al. 2003; Chen et al. 2006). Our finding that both diazoxide and cromakalim decrease single pulse evoked [DA]$_o$ in dorsal striatum provides evidence for expression of functional K$_{ATP}$ channels on DAergic axons. Apparently independent DA release suppression by these channel openers also supports the hypothesis that axonal DA release may be differentially regulated by separate populations of SUR1- and SUR2-based K$_{ATP}$ channels. Whether this might reflect segregation between separate populations of DAergic axons has not yet been determined.

K$_{ATP}$-channel-dependent DA release regulation does not involve altered cholinergic tone

Although DA release elicited by a single pulse is independent from regulation by concurrently released glutamate and GABA (Avshalumov et al. 2003; Chen et al. 2006), tonic ACh release from cholinergic interneurons that are spontaneously active *in vitro* (Bennett and Wilson 1999) exerts a strong modulatory effect on 1 p evoked [DA]$_o$ through activation of nAChRs (Zhou et al. 2001; Rice and Cragg 2004; Zhang and Sulzer 2004). This cholinergic tone facilitates DA release elicited by 1 p stimulation and thereby contributes to a muted frequency dependence of release, which is relieved when nAChRs are blocked (Rice and Cragg 2004; Zhang and Sulzer 2004). Given that striatal cholinergic interneurons express SUR1-based K$_{ATP}$ channels (Lee et al. 1998; Thomzig et al. 2003), it is possible that suppression of 1 p evoked DA release by diazoxide could occur through hyperpolarization of cholinergic neurons and a consequential decrease in ACh tone at nAChRs. However, unlike the enhanced frequency dependence of evoked [DA]$_o$ seen when nAChRs are blocked by mecamylamine, diazoxide suppressed DA release to a similar extent across all frequencies, and thus failed to recreate the dynamic pattern of striatal DA release with frequency that is a hallmark of decreased cholinergic tone. Moreover, additional studies showed that the extent of DA release inhibition by mecamylamine was identical whether applied in the presence or absence of MCS, confirming the lack of involvement of cholinergic interneurons in H$_2$O$_2$-dependent DA release regulation.

Independent regulation of axonal DA release by K$_{ATP}$-channels and D2 autoreceptors

Initial studies of regulation of midbrain DAergic neuron excitability by K$_{ATP}$ channels suggested that these channels and D2 DA autoreceptors might share a common inhibitory mechanism (Roeper et al. 1990; Lin et al. 1993). Similarly, *in vivo* microdialysis studies in

striatum showed that the usual increase in $[DA]_o$ seen with local application of the D2 receptor antagonist sulpiride was prevented by K_{ATP}-channel agents, including cromakalim (Tanaka et al. 1996). However, the mechanism by which this occurs is unclear given that D2 autoreceptors inhibit DA release via GIRK (Uchida et al. 2000) whereas K_{ATP} channels contain their own inward rectifier pore-forming subunits (Clement et al. 1997; Shyng and Nichols 1997). Previous studies of pulse-train evoked $[DA]_o$ in dorsal striatum *in vitro* implied that suppression of evoked DA release by endogenous H_2O_2 was independent of D2 autoreceptor regulation of DA release (Avshalumov and Rice 2003). The present studies using 1 p stimulation demonstrate that activation of K_{ATP} channels and D2R agonists independently regulate axonal DA release in dorsal striatum.

Summary and conclusions

The body of evidence presented here demonstrates that activation of presynaptic K_{ATP} channels on striatal DAergic axons rapidly and selectively inhibits DA release. The time course of activity-dependent release suppression is similar to that seen with D2 autoreceptor regulation of DA release in slices (Lee et al. 2002; Phillips et al. 2002). Like autoreceptor activation, H_2O_2-dependent K_{ATP}-channel opening also contributes to striatal paired-pulse suppression of DA release. In contrast, however, H_2O_2/K_{ATP}-channel-mediated inhibition is a heteroreceptor-dependent process. Subsecond K_{ATP}-channel-dependent regulation is initiated by AMPAR activation in MSNs, with consequent generation of modulatory H_2O_2 that diffuses to target K_{ATP} channels on DAergic axons to inhibit DA release (Avshalumov et al. 2003, 2008). Although K_{ATP} channels on non-DA cells and processes in dorsal striatum might also be activated by dynamically generated H_2O_2, alternative sites, including those on cholinergic interneurons, do not affect DA release. Thus, in the absence of glutamatergic synapses or ionotropic glutamate receptors on DAergic axons (Freund et al. 1984; Smith and Bolam 1990; Bernard et al. 1997; Chen et al. 1998; Bernard and Bolam 1998), H_2O_2-activated K_{ATP} channels on DAergic axons provide a direct target by which corticostriatal and thalamostriatal inputs can modulate DA release.

Acknowledgments

References

Ashcroft SJ, Ashcroft FM. Properties and functions of ATP-sensitive K-channels. Cell Signal. 1990; 2:197–214. [PubMed: 2119205]

Ashcroft FM, Gribble FM. Correlating structure and function in ATP-sensitive K^+ channels. Trends Neurosci. 1998; 21:288–294. [PubMed: 9683320]

Avshalumov MV, Bao L, Patel JC, Rice ME. H_2O_2 signaling in the nigrostriatal dopamine pathway via ATP-sensitive potassium channels: issues and answers. Antioxidants and Redox Signaling. 2007; 9:219–231. [PubMed: 17115944]

Avshalumov MV, Chen BT, Koós T, Tepper JM, Rice ME. Endogenous hydrogen peroxide regulates the excitability of midbrain dopamine neurons via ATP-sensitive potassium channels. J. Neurosci. 2005; 25:4222–4231. [PubMed: 15858048]

Avshalumov MV, Chen BT, Marshall SP, Peña DM, Rice ME. Glutamate-dependent inhibition of dopamine release in striatum is mediated by a new diffusible messenger, H_2O_2. J. Neurosci. 2003; 23:2744–2750. [PubMed: 12684460]

Avshalumov MV, MacGregor DG, Sehgal LM, Rice ME. The glial antioxidant network and neuronal ascorbate: protective yet permissive for H_2O_2 signaling. Neuron Glia Biol. 2004; 1:365–376. [PubMed: 18292802]

Avshalumov MV, Patel JC, Rice ME. AMPA receptor-dependent H_2O_2 generation in striatal spiny neurons, but not dopamine axons: one source of a retrograde signal that can inhibit dopamine release. J. Neurophysiol. 2008; 100:1590–1601. [PubMed: 18632893]

Avshalumov MV, Rice ME. Activation of ATP-sensitive K^+ (K_{ATP}) channels by H_2O_2 underlies glutamate-dependent inhibition of striatal dopamine release. PNAS. 2003; 100:11729–11734. [PubMed: 13679582]

Babenko AP, Gonzalez G, Bryan J. Pharmaco-topology of sulfonylurea receptors. Separate domains of the regulatory subunits of K_{ATP} channel isoforms are required for selective interaction with K^+ channel openers. J. Biol. Chem. 2000; 275:717–720. [PubMed: 10625598]

Bao L, Avshalumov MV, Patel JC, Lee CR, Miller EW, Chang CJ, Rice ME. Mitochondria are the source of hydrogen peroxide for dynamic brain-cell signaling. J. Neurosci. 2009; 29:9002–9010. [PubMed: 19605638]

Bao L, Avshalumov MV, Rice ME. Partial mitochondrial inhibition causes suppression of striatal dopamine release and depolarization of medium spiny neuron via H_2O_2 elevation in the absence of ATP depletion. J. Neurosci. 2005; 25:10029–10040. [PubMed: 16251452]

Bao L, Patel JC, Walker RH, Shashidharan P, Rice ME. Dysregulation of striatal dopamine release in a mouse model of dystonia. J. Neurochem. 2010; 114:1781–1791. [PubMed: 20626557]

Bennett BD, Wilson CJ. Spontaneous activity of neostriatal cholinergic interneurons in vitro. J. Neurosci. 1999; 19:5586–5596. [PubMed: 10377365]

Bernard V, Bolam JP. Subcellular and subsynaptic distribution of the NR1 subunit of the NMDA receptor in the neostriatum and globus pallidus of the rat: colocalization at synapses with the GluR2/3 subunit of the AMPA receptor. Eur. J. Neurosci. 1998; 10:3721–3738. [PubMed: 9875351]

Bernard V, Somogyi P, Bolam JP. Cellular, subcellular, and subsynaptic distribution of AMPA-type glutamate receptor subunits in the neostriatum of the rat. J. Neurosci. 1997; 17:819–833. [PubMed: 8987803]

Calabresi P, Marfia GA, Centonze D, Pisani A, Bernardi G. Sodium influx plays a major role in the membrane depolarization induced by oxygen and glucose deprivation in rat striatal neurons. Stroke. 1999; 30:171–179. [PubMed: 9880406]

Centonze D, Marfia GA, Pisani A, Picconi B, Giacomini P, Bernardi G, Calabresi P. Ionic mechanisms underlying differential vulnerability to ischemia in striatal neurons. Prog. in Neurobiol. 2001; 63:687–696.

Chen BT, Moran KA, Avshalumov MV, Rice ME. Limited regulation of somatodendritic dopamine release by voltage-sensitive Ca^{2+} channels contrasted with strong regulation of axonal dopamine release. J. Neurochem. 2006; 96:645–655. [PubMed: 16405515]

Chen BT, Rice ME. Novel Ca^{2+} dependence and time course of somatodendritic dopamine release: substantia nigra *versus* striatum. J. Neurosci. 2001; 21:7841–7847. [PubMed: 11567075]

Chen Q, Veenman L, Knopp K, Yan Z, Medina L, Song WJ, Surmeier DJ, Reiner A. Evidence for the preferential localization of glutamate receptor-1 subunits of AMPA receptors to the dendritic spines of medium spiny neurons in rat striatum. Neuroscience. 1998; 83:749–761. [PubMed: 9483559]

Clement JP IV, Kunjilwar K, Gonzalez G, Schwanstecher M, Panten U, Aguilar-Bryan L, Bryan J. Association and stoichiometry of K_{ATP} channel subunits. Neuron. 1997; 18:827–838. [PubMed: 9182806]

Cragg SJ. Variable dopamine release probability and short-term plasticity between functional domains of the primate striatum. J. Neurosci. 2003; 23:4378–85. [PubMed: 12764127]

Dunn-Meynell AA, Rawson NE, Levin BE. Distribution and phenotype of neurons containing the ATP-sensitive K^+ channel in rat brain. Brain Res. 1998; 814:41–54. [PubMed: 9838037]

Dunn-Meynell AA, Routh VH, McArdle JJ, Levin BE. Low-affinity sulfonylurea binding sites reside on neuronal cell bodies in the brain. Brain Res. 1997; 745:1–9. [PubMed: 9037388]

Findlay I. Effects of ADP upon the ATP-sensitive K^+ channel in rat ventricular myocytes. J. Membr. Biol. 1988; 101:83–92. [PubMed: 2452884]

Freund TF, Powell JF, Smith AD. Tyrosine hydroxylase-immunoreactive boutons in synaptic contact with identified striatonigral neurons, with particular reference to dendritic spines. Neuroscience. 1984; 13:1189–1215. [PubMed: 6152036]

Glukhov AV, Flagg TP, Fedorov VV, Efimov IR, Nichols CJ. Differential K-$_{ATP}$ channel pharmacology in intact mouse heart. J. Mol. Cell. Cardiology. 2010; 48:152–160.

Ichinari K, Kakei M, Matsuoka T, Nakashima H, Tanaka H. Direct activation of the ATP-sensitive potassium channel by oxygen free radicals in guinea-pig ventricular cells: its potentiation by MgADP. J. Mol. Cell. Cardiol. 1996; 28:1867–1877. [PubMed: 8899545]

Inagaki N, Gonoi T, Clement JP, Wang CZ, Aguilar-Bryan L, Bryan J, Seino S. A family of sulfonylurea receptors determines the pharmacological properties of ATP-sensitive K^+ channels. Neuron. 1996; 16:1011–1017. [PubMed: 8630239]

Isomoto S, Kondo C, Yamada M, Matsumoto S, Higashiguchi O, Horio Y, Matsuzawa Y, Kurachi Y. A novel sulfonylurea receptor forms with BIR (Kir6.2) a smooth muscle type ATP-sensitive K^+ channel. J Biol Chem. 1996; 271:24321–24324. [PubMed: 8798681]

Karschin C, Ecke C, Ashcroft FM, Karschin A. Overlapping distribution of K-ATP channel-forming Kir6.2 subunit and the sulfonylurea receptor SUR1 in rodent brain. FEBS Lett. 1997; 401:59–64. [PubMed: 9003806]

Krippeit-Drews P, Kramer C, Welker S, Lang F, Ammon HPT, Drews G. Interference of H_2O_2 with stimulus-secretion coupling in mouse pancreatic β-cells. J. Physiol. (Lond.). 1999; 514:471–481. [PubMed: 9852328]

Lee K, Dixon AK, Freeman TC, Richardson PJ. Identification of an ATP-sensitive potassium channel current in striatal cholinergic interneurons. J. Physiol. 1998; 510:441–453. [PubMed: 9705995]

Lee TH, Gee KR, Davidson C, Ellinwood EH. Direct, real-time assessment of dopamine release autoinhibition in the rat caudate-putamen. Neuroscience. 2002; 112:647–654. [PubMed: 12074906]

Limberger N, Trout SJ, Kruk ZL, Starke K. "Real time" measurement of endogenous dopamine release during short trains of pulses in slices of rat neostriatum and nucleus accumbens: role of autoinhibition. Naunyn Schmiedebergs Ach Pharmacol. 1991; 344:623–629.

Lin YJ, Greif GJ, Freedman JE. Multiple sulfonylurea-sensitive potassium channels: a novel subtype modulated by dopamine. Mol. Pharmacol. 1993; 44:907–910. [PubMed: 8246912]

Liss B, Bruns R, Roeper J. Alternative sulfonylurea receptor expression defines metabolic sensitivity of K-ATP channels in dopaminergic midbrain neurons. EMBO J. 1999; 18:833–846. [PubMed: 10022826]

Liss B, Haeckel O, Wildmann J, Miki T, Seino S, Roeper J. K-ATP channels promote the differential degeneration of dopaminergic midbrain neurons. Nature Neurosci. 2005; 8:1742–1751. [PubMed: 16299504]

Lu T, Ye D, Wang X, Seubert JM, Graves JP, Bradbury JA, Zeldin DC, Lee HC. Cardiac and vascular K_{ATP} channels in rats are activated by endogenous epoxyeicosatrienoic acids through different mechanisms. J. Physiol. 2006; 575:627–644. [PubMed: 16793897]

Millar J, Pelling CW. Improved methods for construction of carbon fibre electrodes for extracellular spike recording. J. Neuroscience Methods. 2001; 110:1–8.

Morrissey A, Rosner E, Lanning J, Parachuru L, Dhar Chowdhury P, Han S, Lopez G, Tong X, Yoshida H, Nakamura TY, Artman M, Giblin JP, Tinker A, Coetzee WA. Immunolocalization of K_{ATP} channel subunits in mouse and rat cardiac myocytes and the coronary vasculature. BMC Physiol. 2005; 5:1. [PubMed: 15647111]

Mourre C, Ben Ari Y, Bernardi H, Fosset M, Lazdunski M. Antidiabetic sulfonylureas: localization of binding sites in the brain and effects on the hyperpolarization induced by anoxia in hippocampal slices. Brain Res. 1989; 486:159–164. [PubMed: 2497930]

Nichols CG. K_{ATP} channels as molecular sensors of cellular metabolism. Nature. 2006; 440:470–476. [PubMed: 16554807]

Noma A. ATP-regulated K^+ channels in cardiac muscle. Nature. 1983; 305:147–148. [PubMed: 6310409]

Patel, J.; Rice, ME. Dopamine Release in Brain Slices. In: Grimes, CA.; Dickey, EC.; Pishko, MV., editors. Encyclopedia of Sensors. Vol. 6. American Scientific Publishers, Stevenson Ranch; California, USA: 2006. p. 313-334.

Patel J, Trout SJ, Kruk ZL. Regional differences in evoked dopamine efflux in brain slices of rat anterior and posterior caudate putamen. Naunyn Schmiedebergs Arch. Pharmacol. 1992; 346:267–276. [PubMed: 1407013]

Patel JC, Witkovsky P, Avshalumov MV, Rice ME. Mobilization of calcium from intracellular stores facilitates somatodendritic dopamine release. J. Neurosci. 2009; 29:6568–6579. [PubMed: 19458227]

Phillips PEM, Hancock PJ, Stamford JA. Time window of autoreceptor-mediated inhibition of limbic and striatal dopamine release. Synapse. 2002; 44:15–22. [PubMed: 11842442]

Rice ME, Cragg SJ. Nicotine amplifies reward-related dopamine signals in striatum. Nature Neurosci. 2004; 7:583–584. [PubMed: 15146188]

Rice ME, Cragg SJ, Greenfield SA. Characteristics of electrically evoked somatodendritic dopamine release in substantia nigra and ventral tegmental area in vitro. J. Neurophysiol. 1997; 77:853–862. [PubMed: 9065854]

Roeper J, Hainsworth AH, Ashcroft FM. Tolbutamide reverses membrane hyperpolarizations induced by activations of D_2 receptors in isolated substantia nigra neurons. Pflugers Arch. 1990; 416:473–475. [PubMed: 2169045]

Schwanstecher C, Panten U. Identification of an ATP-sensitive K^+ channel in spiny neurons of rat caudate nucleus. Pflugers Arch. 1994; 427:187–199. [PubMed: 8058471]

Shyng S, Nichols CG. Octameric stoichiometry of the K_{ATP} channel complex. J. Gen. Physiol. 1997; 110:655–664. [PubMed: 9382894]

Shyng S-L, Ferrigni T, Nichols CG. Regulation of K_{ATP} channel activity by diazoxide and MgADP: distinct functions of the nucleotide binding folds of the sulphonylurea receptor. J. Gen. Physiol. 1997; 110:643–654. [PubMed: 9382893]

Smith AD, Bolam JP. The neural artwork of the basal ganglia as revealed by the study of synaptic connections of identified neurons. Trends Neurosci. 1990; 13:259–265. [PubMed: 1695400]

Tanaka T, Yoshida M, Yokoo H, Mizoguchi K, Tanaka M. ATP-sensitive K^+ channel openers block sulpiride-induced dopamine release in the rat striatum. Eur. J. Pharmacol. 1996; 297:35–41. [PubMed: 8851163]

Thomzig A, Wenzel M, Karschin C, Eaton MJ, Skatchkov SN, Karschin A, Veh RW. Kir6.1 is the principal pore-forming subunit of astrocyte but not neuronal plasma membrane K-ATP channels. Mol. Cell. Neurosci. 2001; 18:671–690. [PubMed: 11749042]

Thomzig A, Prüss H, Veh RW. The Kir6.1-protein, a pore-forming subunit of ATP-sensitive potassium channels, is prominently expressed by giant cholinergic interneuron in the striatum of the rat brain. Brain Research. 2003; 986:132–138. [PubMed: 12965237]

Tokube K, Kiyosue T, Arita M. Effects of hydroxyl radicals on K_{ATP} channels in guinea-pig ventricular myocytes. Pflugers Arch. 1998; 437:155–157. [PubMed: 9817800]

Treherne JM, Ashford ML. The regional distribution of sulphonylurea binding sites in rat brain. Neuroscience. 1991; 40:523–531. [PubMed: 1902917]

Trout SJ, Kruk ZL. Differences in evoked dopamine efflux in rat caudate putamen, nucleus accumbens and tuberculum olfactorium in the absence of uptake inhibition: influence of autoreceptors. Br. J. Pharmacol. 1992; 106:452–458. [PubMed: 1393270]

Uchida S, Akaike N, Nabekura J. Dopamine activates inward rectifier K^+ channel in acutely dissociated rat substantia nigra neurons. Neuropharmacology. 2000; 39:191–201. [PubMed: 10670414]

Witkovsky P, Patel JC, Lee CR, Rice ME. Immunocytochemical identification of proteins involved in dopamine release from the somatodendritic compartment of nigral dopaminergic neurons. Neuroscience. 2009; 164:488–496. [PubMed: 19682556]

Xia Y, Haddad GG. Major differences in CNS sulfonylurea receptor distribution between the rat (newborn, adult) and turtle. J. Comp. Neurol. 1991; 314:278–289. [PubMed: 1787178]

Zhang H, Sulzer D. Frequency-dependent modulation of dopamine release by nicotine. Nature Neurosci. 2004; 7:581–582. [PubMed: 15146187]

Zhou FM, Liang Y, Dani JA. Endogenous nicotinic cholinergic activity regulates dopamine release in striatum. Nature Neurosci. 2001; 4:1224–1229. [PubMed: 11713470]

Zini S, Tremblay E, Pollard H, Moreau J, Ben-Ari Y. Regional distribution of sulfonylurea receptors in the brain of rodent and primate. Neuroscience. 1993; 55:1085–1091. [PubMed: 8232899]
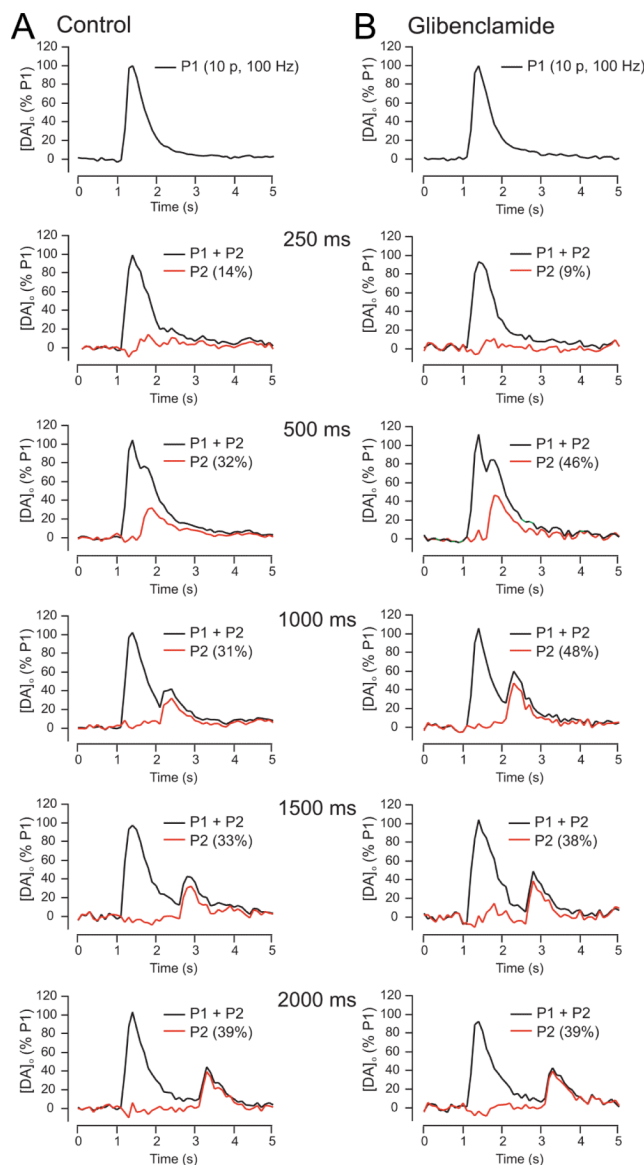
Figure 1. Paired-pulse stimulation paradigm used to reveal the time course of K_{ATP}-channel activation by endogenous H_2O_2

A. Representative $[DA]_o$ *versus* time records from paired-pulse stimulation in striatal slices showing the effect of a pseudo-one-pulse stimulus (10 pulses, 100 Hz; P1) followed by a single test pulse (P2), applied at varying intervals (P1+P2, black traces). The amplitude of $[DA]_o$ evoked by P2 is seen for each interval when P1 is subtracted from P1+P2 (red traces). Note the recovery of P2 amplitude with time. **B.** Similar records obtained in glibenclamide (3 μM), a selective K_{ATP}-channel blocker, show increases in P2 evoked $[DA]_o$ between 500 ms and 1500 ms (see Fig. 2). All recordings were made in (−)sulpiride (1 μM) to prevent inhibition of DA release via D_2 autoreceptors.
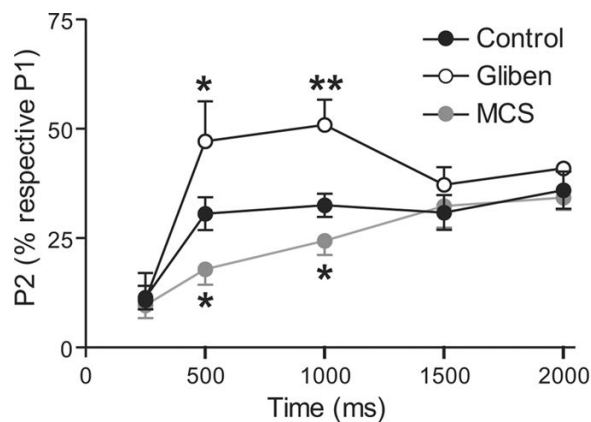
Figure 2. Time frame for regulation of axonal DA release by endogenous H_2O_2 and K_{ATP} channels is rapid and transient

Mean data showing the time-course of the recovery in amplitude of $[DA]_o$ evoked by P2 (1 p) relative to P1 (10 p, 100 Hz) when applied with increasing interval from P1 under control conditions (n = 8–12 for each time point) in the presence of the selective K_{ATP}-channel blocker glibenclamide (Gliben, 3 μM) or in mercaptosuccinate (MCS, 1 mM), a GSH peroxidase inhibitor. Glibenclamide significantly increased $[DA]_o$ evoked by P2 at 500 ms (n = 5, *$p < 0.05$ *vs*, control, *t*-test) and 1000 ms (n = 5, **$p < 0.01$ *vs*. control, *t*-test), thereby unmasking a role for K_{ATP}-channel activation following the initial P1 stimulation. By contrast MCS significantly decreased $[DA]_o$ evoked by P2 at 500 ms (n = 7, *$p < 0.05$ *vs*. control, *t*-test) and 1000 ms (n = 7, *$p < 0.05$ *vs*. control, *t*-test), revealing a role for endogenous H_2O_2 generated during the initial P1 stimulation. All recordings were made in (−)sulpiride (1 μM) to prevent any inhibition of DA release via D_2 autoreceptors. Data sets were analyzed using two-way ANOVA for comparison of glibenclamide *versus* control ($p < 0.01$) or MCS *versus* control ($p = 0.05$).
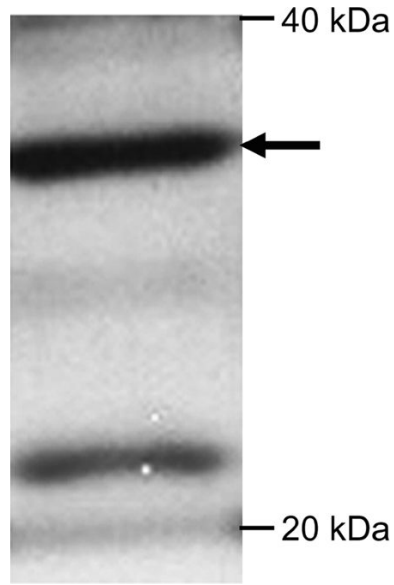
Figure 3. Western blot of guinea-pig striatum stained with C62 anti-Kir6.2
A primary band is seen at 37 kD (arrow) corresponding to the molecular mass of Kir6.2. A secondary band is visible at 22 kD.
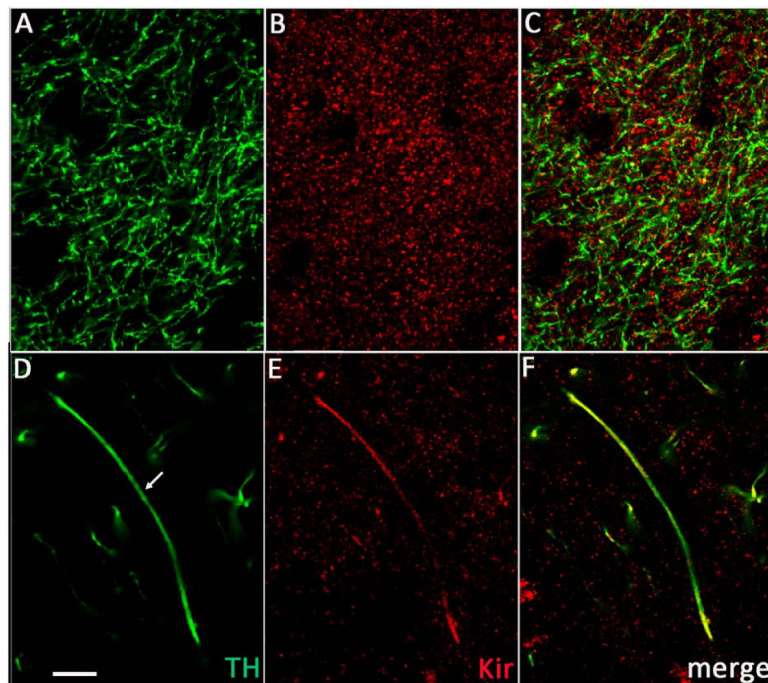
Figure 4. Colocalization of Kir6.2 (Kir) and tyrosine hydroxylase (TH) immunoreactivities in striatum
A–C. Section of guinea-pig dorsal striatum from a region with highly branched DAergic axons immunostained for **(A)** TH and **(B)** Kir6.2 using LL anti-Kir6.2 antibody; **(C)** merged image. **D**–**F**. Another section of guinea-pig striatum containing an extended DAergic axon immunostained for **(D)** TH and **(E)** Kir6.2 using NBP1-00900 anti-Kir6.2 antibody; **(F)** merged image. Note the broad distribution of Kir6.2-ir puncta throughout the striatum **(B and E)**. Scale bar in **(D)** is 10 μm and applies to all panels.
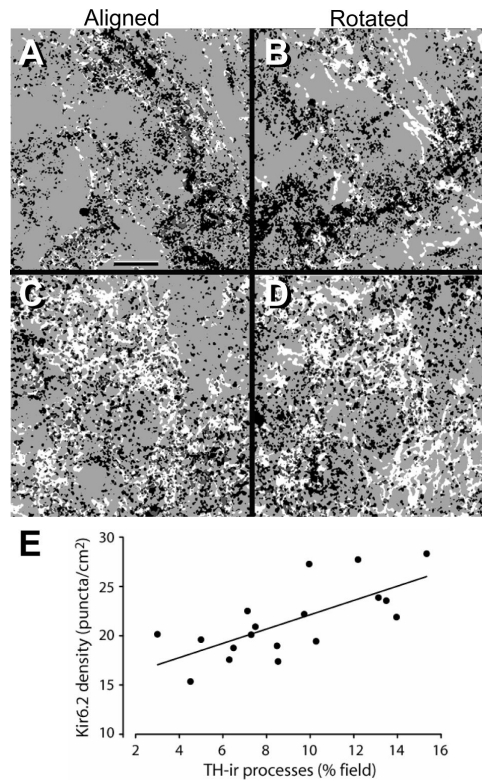
Figure 5. Image rotation confirms localization of Kir6.2 in striatal DAergic axons
A. Representative aligned superimposed fields from a section of guinea-pig striatum immunostained using C62 anti-Kir6.2 with anti-TH. In all panels, TH-ir profiles are white; Kir6.2-ir puncta that colocalize with a TH-ir profile are gray; Kir6.2-ir puncta that do not colocalize with TH-ir profiles are black. **B.** Rotation of the Kir6.2-ir image from **(A)** 90° clockwise markedly decreased the degree of colocalization. **C,D.** Another example of aligned and rotated merged immunostained images using NBP1-00900 anti-Kir6.2 with anti-TH. Scale bar in **(A)** is 10 μm and applies to all panels. See Table 1 for quantitative analysis of several superimposed aligned and rotated fields. **E.** Plot of Kir-6.2-ir density *versus* the percent occupancy of the field of TH-ir processes from 6 separate striatal sections is positively correlated ($r^2 = 0.49$) providing further evidence for colocalization.
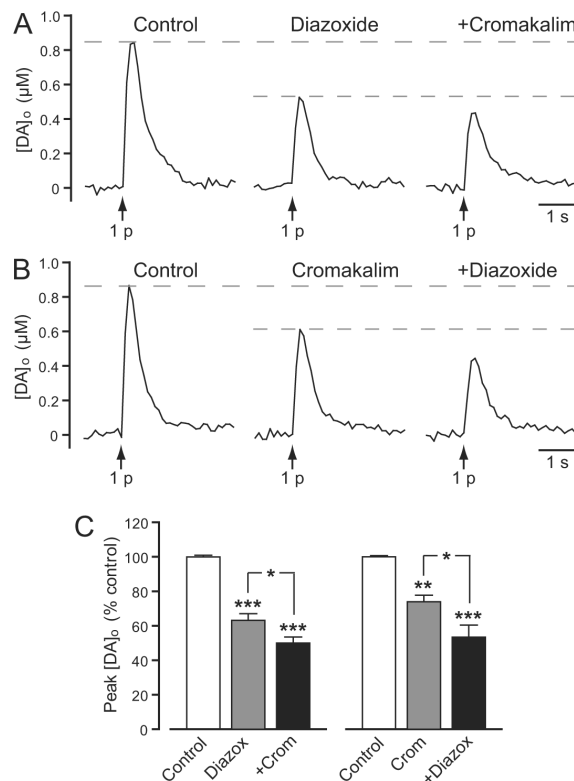
**Figure 6. Presynaptic K_{ATP} channels suppress axonal DA release**
A and B. Representative $[DA]_o$ *versus* time records obtained in striatal slices showing the effect of SUR1 and SUR2 K_{ATP}-channel openers on DA release evoked by local single-pulse stimulation (1 p). **A.** Representative records of 1 p evoked $[DA]_o$ in control conditions, in the presence of the SUR1-acting K_{ATP}-channel opener diazoxide (60 μM) and in the presence of diazoxide plus the SUR2-acting K_{ATP}-channel opener cromakalim (60 μM). **B.** Representative records of 1 p evoked $[DA]_o$ in control conditions, in the presence of cromakalim (30 μM) and in the presence of cromakalim plus diazoxide (30 μM). **C.** Mean data for the effect of K_{ATP}-channel openers on peak $[DA]_o$ evoked by 1 p. Diazoxide (Diazox; 30–60 μM) decreased peak $[DA]_o$ by ~38% (***$p < 0.001$ *vs.* control); a further decrease was seen when cromakalim (Crom; 30–60 μM) was co-applied (*$p < 0.05$ *vs.* diazoxide alone) (n = 6). Cromakalim (30–60 μM) decreased peak $[DA]_o$ by ~26% (**$p < 0.01$ *vs.* control); a further decrease was seen when diazoxide (30–60 μM) was co-applied (*$p < 0.05$ *vs.* cromakalim alone) (n = 6). Data were analyzed using one-way ANOVA with Bonferroni's multiple comparisons of selected sets.
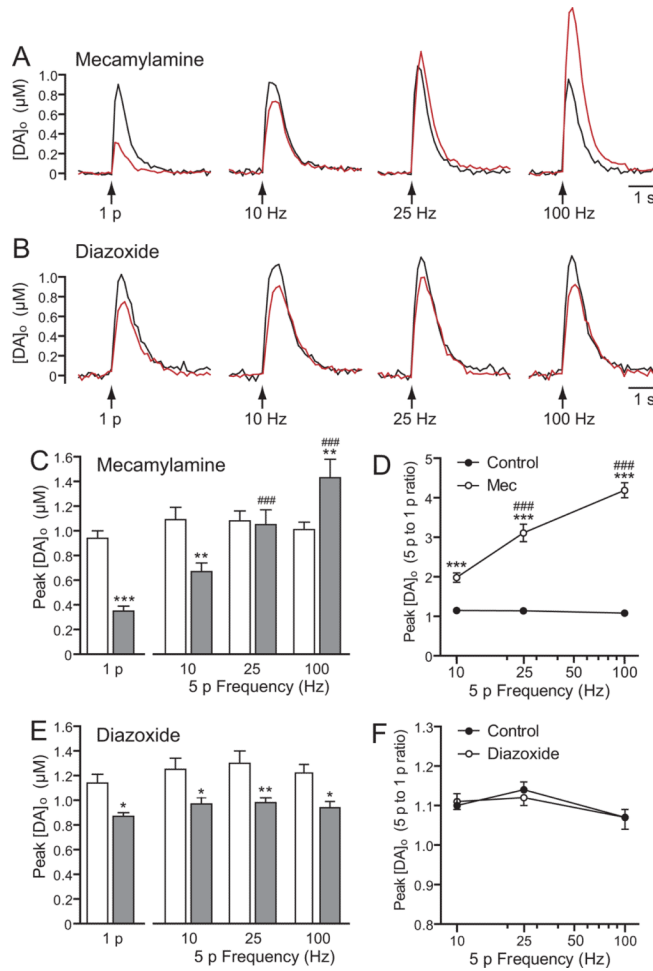
Figure 7. Suppression of axonal DA release by SUR1-based K$_{ATP}$-channels does not occur via decreased cholinergic tone at nAChRs

A and B. Representative 1 p and 5 p evoked [DA]$_o$ recorded in striatal slices in the absence (black traces) and presence (red traces) of mecamylamine (500 nM), a nAChR antagonist **(A)** or diazoxide (60 μM), a SUR1-selective K$_{ATP}$-channel opener **(B). C.** Mean data for the effect of mecamylamine on peak [DA]$_o$ evoked by 1 p or 5 p (Mec, n = 9 recording sites) showing suppression of [DA]$_o$ evoked by 1 p and 5 p at 10 Hz, maintenance of release with 5 p at 25 Hz, and enhancement of peak [DA]$_o$ evoked with 5 p at 100 Hz (**$p < 0.01$, ***$p < 0.001$ *vs.* control; two-way ANOVA with Bonferroni's post-hoc analysis). Consequently, in mecamylamine peak [DA]$_o$ evoked by 5 p at   25 Hz was significantly higher than that evoked by 1 p (###$p < 0.001$ *vs.* respective 1 p evoked [DA]$_o$,; one-way ANOVA with Dunnett's multiple comparisons). **D.** Ratio of 5 p to 1 p evoked [DA]$_o$ showing an enhanced frequency-dependence in the presence of mecamylamine (n = 9 recording sites; **$p < 0.01$; ***$p < 0.001$ *vs.* control, twoway ANOVA with Bonferroni's post-hoc analysis; ###$p < 0.001$ *vs.* respective 10 Hz evoked [DA]$_o$; one-way ANOVA with Dunnett's multiple comparisons). **E.** Mean data for the effect of diazoxide on peak [DA]$_o$ evoked by 1 p or 5 p (n = 9 recording sites) showing a similar suppression of peak [DA]$_o$ evoked by 1 p and 5 p at all stimulation frequencies (*$p < 0.05$;**$p < 0.01$ *vs.* control; two-way ANOVA with Bonferroni's post-hoc analysis). **F.** Ratio of 5 p to 1 p evoked [DA]$_o$ across frequencies was unaltered by diaxoxide (n = 9 recording sites; $p > 0.05$ *vs.* control at all frequencies; two-way ANOVA with Bonferroni's post-hoc analysis).
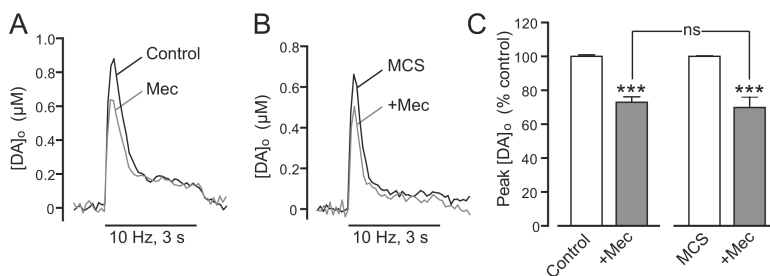
Figure 8. Suppression of axonal DA release by endogenous H_2O_2 does not occur via decreased cholinergic tone at nAChRs

A and B. Representative $[DA]_o$ *versus* time records evoked by pulse-train stimulation (30 pulses at 10 Hz) obtained with the nAChR antagonist mecamylamine (Mec, 5 µM) in control conditions **(A)** or in the presence of the GSH peroxidase inhibitor mercaptosuccinate acid (MCS, 1 mM) **(B). C.** Mean data for the effect of mecamylamine on peak $[DA]_o$ evoked by 30 p in the absence and presence of MCS. Data are normalized, with each respective control peak evoked $[DA]_o$ taken as 100%. Mecamylamine decreased evoked $[DA]_o$ by ~30% under control conditions (n = 5, ****p* < 0.001 *versus* in control). This decrease was similar to that observed when endogenous H_2O_2 levels were enhanced by inhibition of GSH peroxidase with MCS (n = 5, ****p* < 0.001 *versus* in MCS alone). Data were analyzed using one-way ANOVA with Bonferroni's post-hoc analysis.
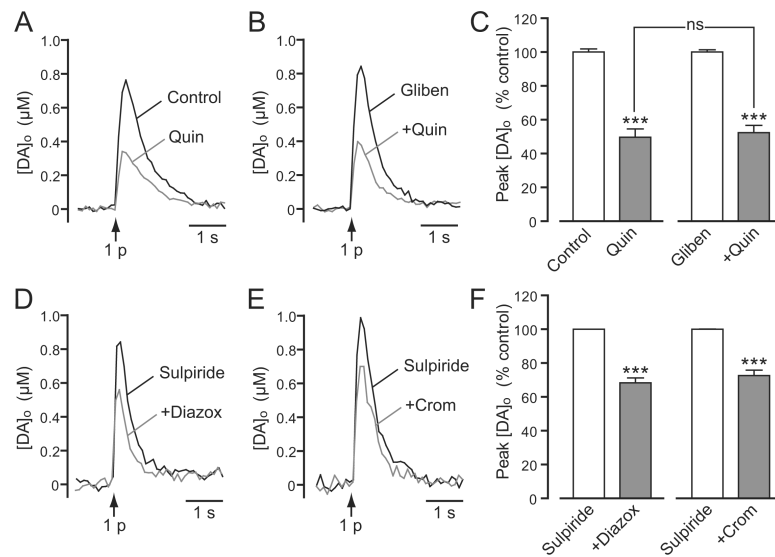
Figure 9. Independence of DA release inhibition by D2 autoreceptors and K_{ATP} channels
A,B. Representative $[DA]_o$ *versus* time records showing the effect of **(A)** quinpirole (Quin, 100 nM) alone and **(B)** in the presence of glibenclamide (Gliben, 3–10 µM) on single-pulse (1 p) evoked $[DA]_o$ in guinea-pig striatal slices. **C.** Mean data for the effect of quinpirole on 1 p evoked peak $[DA]_o$ under control conditions (n = 5, ***$p < 0.001$ *vs.* control), and with glibenclamide (n = 6, ***$p < 0.001$ *vs.* glibenclamide alone). Quinpirole caused a similar ~50% suppression of DA release in the absence and presence of glibenclamide ($p > 0.05$ *vs.* quinpirole alone, one-way ANOVA with Bonferroni's multiple comparisons of selected sets). **D,E.** Representative $[DA]_o$ *versus* time records showing the effect of **(D)** diazoxide (Diazox, 60 µM) and **(E)** cromakalim (Crom, 60 µM) on 1 p evoked DA release in the presence of sulpiride (2 µM). **F.** Mean data for the effect of these SUR-selective K_{ATP}-channel openers on peak $[DA]_o$ evoked by 1 p in sulpiride. Both diazoxide and cromakalim caused the usual ~30% decrease in peak $[DA]_o$ of when D2Rs were blocked (n = 6, ***$p < 0.001$ *vs.* sulpiride alone, one-way ANOVA with Bonferroni's multiple comparisons of selected sets).

Table 1

Colocalization of Kir6.2 and TH in striatum

Field	Aligned *(count)*	90° rotation *(count)*	Difference *(count)*
1	100% *(3765)*	70.8% *(2667)*	−29.2% *(−1098)*
2	100% *(870)*	68.3% *(594)*	−31.7% *(−275)*
3	100% *(1953)*	75.7% *(1479)*	−24.3% *(−474)*
4	100% *(2606)*	69.5% *(1812)*	−30.5% *(−794)*
5	100% *(2675)*	67.6% *(1808)*	−32.4% *(−867)*
6	100% *(2000)*	71.5% *(1429)*	−28.5% *(−571)*
Mean difference			−29.4 ± 2.9% [**]

[**] $p < 0.01$ for Kir6.2 and TH colocalization in aligned superimposed fields *versus* fields with 90° rotation of Kir6.2 immunostaining (see also Fig. 5).